Low-lying states of two-dimensional double-well potentials

2005 J. Phys. A: Math. Gen. 38 2189

(http://iopscience.iop.org/0305-4470/38/10/010)

INSTITUTE OF PHYSICS PUBLISHING JOURNAL OF PHYSICS A: MATHEMATICAL AND GENERAL

J. Phys. A: Math. Gen. **38** (2005) 2189–2199 doi:10.1088/0305-4470/38/10/010

Low-lying states of two-dimensional double-well potentials

Amlan K Roy[1], **Ajit J Thakkar**[1] **and B M Deb**[2,3]

[1] Department of Chemistry, University of New Brunswick, Fredericton, NB E3B 6E2, Canada
[2] Theoretical Chemistry Group, Department of Chemistry, Punjab University, Chandigarh 160 014, India

Received 14 September 2004, in final form 7 January 2005
Published 23 February 2005
Online at stacks.iop.org/JPhysA/38/2189

Abstract

Wavefunctions, energies and selected expectation values of the low-lying stationary states of two-dimensional double-well potentials are obtained from the long-time solutions of the corresponding time-dependent Schrödinger equation. The numerical method consists of transformation to a diffusion-like equation which is then solved by an alternating-direction, implicit, finite-difference method. The method is tested for cases in which the energies have been obtained by other methods. Then the dependence of the energies and other properties on the potential parameters is discussed on the basis of results for four states of 35 different sets of potential parameters including some that lead to pseudo-degeneracies.

PACS numbers: 03.65.Ge, 02.70.Bf, 02.60.Lj, 33.20.−t

1. Introduction

A double-well oscillator is described by a potential function that has two minima separated by a barrier. Problems which are modelled with the help of double-well potentials include the inversion of ammonia, tunnelling of protons in hydrogen bonded systems, structural phase transitions and quantum coherence in Josephson junction superconductors. Thus, it is not surprising that one-dimensional quantum systems with double-well potentials, particularly the anharmonic potential function $V(x) = -Z^2x^2 + \lambda x^4$, have been studied extensively since the pioneering work of Hund [1].

Relatively little work has been done on double-well potentials in two and three dimensions. Progress on the computation of energy levels for such potentials has been made by Witwit and co-workers using inner product perturbation theory and the Hill determinant approach [2–9]. Most of that work has focused on symmetric potentials although nonsymmetric potentials

[3] From October 2004: S N Bose National Centre for Basic Sciences, JD Block, Sector III, Salt Lake, Kolkata 700 098, India.

have also been considered. However, wavefunctions and properties other than the energy remain unexamined to our knowledge. In this work, we use a finite-difference method to examine energies, wavefunctions and properties of the four lowest states of two-dimensional double-well potentials given by

$$V(x, y) = -Z_x^2 x^2/2 - Z_y^2 y^2/2 + \lambda(a_{xx}x^4 + 2a_{xy}x^2y^2 + a_{yy}y^4)/2. \tag{1}$$

The general theory behind the method of solution, which is quite different from the methods used so far for this problem, is outlined in section 2, the numerical method used is detailed in section 3, the results are presented and discussed in section 4 and a few concluding remarks are made in section 5. Atomic units ($\hbar = m_e = e = 1$) are used throughout.

2. Theory

The quantities of interest are solutions of the time-independent Schrödinger equation

$$\hat{H}\phi_{j,k}(x, y) = E_{j,k}\phi_{j,k}(x, y), \tag{2}$$

where the time-independent Hamiltonian is given by

$$\hat{H} = -\tfrac{1}{2}\left(D_x^2 + D_y^2\right) + V(x, y) \tag{3}$$

in which $D_x^2 = \partial^2/\partial x^2$, $D_y^2 = \partial^2/\partial y^2$, the potential V is given by equation (1), and two quantum numbers $\{j \geqslant 0, k \geqslant 0\}$ are used to label the solutions of the two-dimensional Schrödinger equation (2). In this work, we find the stationary state wavefunctions $\phi_{j,k}(x, y)$ as long-time limits of solutions of the time-dependent Schrödinger equation:

$$\hat{H}\psi(x, y; t) = \mathrm{i}\frac{\partial\psi(x, y; t)}{\partial t}, \tag{4}$$

where $\hat{H}$ is the time-independent Hamiltonian of equation (3). As in previous work [10, 11], we write equation (4) in imaginary time τ instead of real time t, then replace τ by $\tau = -\mathrm{i}t$, and finally let $D_t = \partial/\partial t$, to obtain a diffusion-like equation

$$\hat{H}\psi(x, y; t) = -D_t\psi(x, y; t) \tag{5}$$

or simply $\hat{H} = -D_t$ in operator form. Equation (5) resembles a diffusion quantum Monte Carlo equation. One may express $\psi(x, y; t)$ as [12]

$$\psi(x, y; t) = C_{0,0}\phi_{0,0}(x, y) + \sum_{j,k>0}^{\infty} C_{j,k}\phi_{j,k}(x, y)\,\mathrm{e}^{-(E_{j,k}-E_{0,0})t} \tag{6}$$

from which it is apparent that

$$\lim_{t\to\infty}\psi(x, y; t) = C_{0,0}\phi_{0,0}(x, y) \tag{7}$$

so that numerically propagating $\psi(x, y; t)$ to a sufficiently long time t will give us the ground state time-independent wavefunction apart from a normalization constant. Expectation values of properties, including the energy, can be obtained as mean values of the pertinent operator $\hat{A}$:

$$\langle A\rangle = \lim_{t\to\infty}\langle\psi(x, y; t)|\hat{A}\psi(x, y; t)\rangle, \tag{8}$$

where the angular brackets indicate integration over the entire domain of the spatial variables $\{x, y\}$. Excited states can be treated in the same way provided that one ensures they stay orthogonal to all lower states at each time step. This method is applicable to cases where some time-independent methods may not work well, and can equally be used for propagation in imaginary time. It has been applied previously to one-dimensional anharmonic, double-well

and self-interacting oscillators [13–15]. Expectation values of multiplicative operators could also be computed using an energy shift method [16]. An alternative to our method is direct use of the time-dependent Schrödinger equation [17] which has given rise to the widely used method of filter diagonalization.

3. Numerical methods

Now consider the numerical solution of equation (5). Time propagation of $\psi(x, y; t)$ can be expressed in terms of the Taylor expansion of $\psi(x, y; t_0 + \Delta t)$ around t_0 given by

$$\psi(x, y; t_0 + \Delta t) = \lim_{t \to t_0} \left[1 + \Delta t D_t + \frac{(\Delta t)^2}{2!} D_t^2 + \cdots \right] \psi(x, y; t)$$
$$= \lim_{t \to t_0} \mathrm{e}^{\Delta t D_t} \psi(x, y; t) = \lim_{t \to t_0} \mathrm{e}^{-\Delta t \hat{H}} \psi(x, y; t), \tag{9}$$

where $\hat{H} = -D_t$ has been used. The evolution operator $\mathrm{e}^{-\Delta t \hat{H}}$ is not unitary, and hence $\psi(x, y; t_0 + \Delta t)$ may not be normalized even if $\psi(x, y; t_0)$ was normalized.

A uniform temporal grid is defined by $t_n = n\Delta t$ so that $\mathrm{e}^{-\Delta t \hat{H}}$ can be used for each time step. A uniform $N_x \times N_y$ grid, symmetrically laid out around the origin, is defined for the two spatial coordinates as follows:

$$x_\ell = x_1 + (\ell - 1)h_x, \qquad \ell = 1, 2, \ldots, N_x \tag{10}$$

$$y_m = y_1 + (m - 1)h_y, \qquad m = 1, 2, \ldots, N_y, \tag{11}$$

where $x_1 = -h_x(N_x - 1)/2$, $y_1 = -h_y(N_y - 1)/2$ and both N_x and N_y are odd integers. Using notation defined by $\psi^n_{\ell,m} = \psi(x_\ell, y_m; t_n)$, equation (9) can be written on this discrete grid as

$$\psi^{n+1}_{\ell,m} = \mathrm{e}^{-\Delta t \hat{H}_{\ell,m}} \psi^n_{\ell,m} \tag{12}$$

or, in symmetric form, as

$$\mathrm{e}^{(\Delta t/2)\hat{H}_{\ell,m}} \psi^{n+1}_{\ell,m} = \mathrm{e}^{-(\Delta t/2)\hat{H}_{\ell,m}} \psi^n_{\ell,m}. \tag{13}$$

Partitioning the Hamiltonian of equation (3) into two components

$$\hat{H} = \tfrac{1}{2}(\hat{H}^x + \hat{H}^y), \tag{14}$$

where

$$\hat{H}^a = -D_a^2 + V(x, y), \qquad \text{for} \quad a = x, y, \tag{15}$$

and substituting equation (14) into equation (13) yields

$$\left[\mathrm{e}^{(\Delta t/4)\hat{H}^x_{\ell,m}} \times \mathrm{e}^{(\Delta t/4)\hat{H}^y_{\ell,m}}\right] \psi^{n+1}_{\ell,m} = \left[\mathrm{e}^{-(\Delta t/4)\hat{H}^x_{\ell,m}} \times \mathrm{e}^{-(\Delta t/4)\hat{H}^y_{\ell,m}}\right] \psi^n_{\ell,m}. \tag{16}$$

Expanding the exponentials in Taylor series and retaining only the first two terms lead to

$$\left(1 + \frac{\Delta t}{4}\hat{H}^x_{\ell,m}\right)\left(1 + \frac{\Delta t}{4}\hat{H}^y_{\ell,m}\right)\psi^{n+1}_{\ell,m} = \left(1 - \frac{\Delta t}{4}\hat{H}^x_{\ell,m}\right)\left(1 - \frac{\Delta t}{4}\hat{H}^y_{\ell,m}\right)\psi^n_{\ell,m}. \tag{17}$$

A cancellation of errors is likely in equation (17) because discretization and truncation errors occur on both sides.

Next we split equation (17) with the Peaceman–Rachford scheme [18]. This is an unconditionally stable, convergent, alternating-direction (AD), implicit (I), finite-difference method which is accurate to second order in Δt, h_x and h_y [19]. Such ADI finite-difference methods have a long history; an early application to a time-dependent Schrödinger equation was made by Deb and Chattaraj [20]. The splitting leads to the replacement of equation (17)

by the two-step difference scheme

$$\left(1+\frac{\Delta t}{4}\hat{H}^{x}_{\ell,m}\right)\psi^{n+1/2}_{\ell,m}=\left(1-\frac{\Delta t}{4}\hat{H}^{y}_{\ell,m}\right)\psi^{n}_{\ell,m}, \tag{18}$$

$$\left(1+\frac{\Delta t}{4}\hat{H}^{y}_{\ell,m}\right)\psi^{n+1}_{\ell,m}=\left(1-\frac{\Delta t}{4}\hat{H}^{x}_{\ell,m}\right)\psi^{n+1/2}_{\ell,m}, \tag{19}$$

where $\psi^{n+1/2}_{\ell,m}$ is a non-physical function bridging $\psi^{n}_{\ell,m}$ and $\psi^{n+1}_{\ell,m}$. Next we approximate D_x^2 and D_y^2 by three-point, finite-difference formulae [21] as

$$D_x^2\psi^{n}_{\ell,m}=h_x^{-2}\left(\psi^{n}_{\ell+1,m}-2\psi^{n}_{\ell,m}+\psi^{n}_{\ell-1,m}\right) \tag{20}$$

and

$$D_y^2\psi^{n}_{\ell,m}=h_y^{-2}\left(\psi^{n}_{\ell,m+1}-2\psi^{n}_{\ell,m}+\psi^{n}_{\ell,m-1}\right). \tag{21}$$

Then we find that equation (18) can be written as N_y symmetric, tridiagonal sets of N_x linear equations

$$-c_x\left(\psi^{n+1/2}_{\ell-1,m}+\psi^{n+1/2}_{\ell+1,m}\right)+(1+\alpha_{\ell,m})\psi^{n+1/2}_{\ell,m}=\xi^{n}_{\ell,m}, \tag{22}$$

where

$$\xi^{n}_{\ell,m}=(1-\beta_{\ell,m})\psi^{n}_{\ell,m}+c_y\left(\psi^{n}_{\ell,m-1}+\psi^{n}_{\ell,m+1}\right), \tag{23}$$

$$\alpha_{\ell,m}=2c_x+V_{\ell,m}\Delta t/4, \tag{24}$$

$$\beta_{\ell,m}=2c_y+V_{\ell,m}\Delta t/4 \tag{25}$$

and

$$c_a=\frac{\Delta t}{4h_a^2},\qquad a\in\{x,y\}. \tag{26}$$

Similarly, equation (19) can be written as N_x symmetric, tridiagonal sets of N_y linear equations

$$-c_y\left(\psi^{n+1}_{\ell,m-1}+\psi^{n+1}_{\ell,m+1}\right)+(1+\beta_{\ell,m})\psi^{n+1}_{\ell,m}=\zeta^{n}_{\ell,m}, \tag{27}$$

where

$$\zeta^{n}_{\ell,m}=(1-\alpha_{\ell,m})\psi^{n+1/2}_{\ell,m}+c_x\left(\psi^{n+1/2}_{\ell-1,m}+\psi^{n+1/2}_{\ell+1,m}\right). \tag{28}$$

The overall solution procedure can now be specified as follows:

(i) Set $n=0$. Generate an initial guess for the wavefunction ψ^0 at $t_0=0$. If an excited state is being sought, orthogonalize ψ^0 to all lower states by the Gram–Schmidt method [22]. Normalize ψ^0 and calculate its energy $E^0=\langle\psi^0|\hat{H}\psi^0\rangle$.

(ii) For each fixed $m=2,3,\ldots,N_y-1$, solve equation (22) with $\ell=2,3,\ldots,N_x-1$ by LU decomposition [22] to obtain $\psi^{n+1/2}_{\ell,m}$ on the entire grid excluding the four edges of the enclosing rectangle with vertices at $(\pm x_1,\pm y_1)$. Then generate $\psi^{n+1/2}_{\ell,m}$ on the perimeter of the rectangle.

(iii) For each fixed $\ell=2,3,\ldots,N_x-1$, solve equation (27) with $m=2,3,\ldots,N_y-1$ by LU decomposition [22] to obtain $\psi^{n+1}_{\ell,m}$ on the entire grid excluding the perimeter. Then generate $\psi^{n+1}_{\ell,m}$ on the perimeter of the rectangle.

(iv) If an excited state is being sought, orthogonalize ψ^{n+1} to all lower states by the Gram–Schmidt method [22]. Normalize ψ^{n+1} and calculate its energy $E^{n+1}=\langle\psi^{n+1}|\hat{H}\psi^{n+1}\rangle$.

(v) Check for convergence to the long-time limit by checking $|E^{n+1}-E^n|\leqslant\epsilon$ where ϵ is a convergence threshold which was chosen to be 10^{-12} in this work. If this condition is

satisfied, proceed to the next step. Otherwise increment n by 1 and take another time step by looping back to step (ii) of the computational procedure.

(vi) Calculate other properties of interest from the converged wavefunction.

The points on the perimeter of the rectangle were obtained by three-point extrapolation [21]. However, setting them to zero was found to be equally good provided that the rectangle was large enough.

The energy and overlap integrals needed at each time step were calculated by Simpson's rule, a three-point Newton–Cotes quadrature. The integrals for the energy and other properties from the converged wavefunction were calculated with a seven-point Newton–Cotes quadrature [21]. The latter procedure requires that N_x and N_y be of the form $6k + 1$.

The kinetic component, T, of the energy was computed from

$$T = (1/2)(\langle D_x\phi|D_x\phi\rangle + \langle D_y\phi|D_y\phi\rangle) \tag{29}$$

rather than

$$T = -(1/2)\left(\left\langle\phi\middle|D_x^2\phi\right\rangle + \left\langle\phi\middle|D_x^2\phi\right\rangle\right) \tag{30}$$

to avoid numerical second derivatives. A five-point, finite-difference formula [21] was used to obtain the first derivatives in equation (29).

4. Results and discussion

We begin by discussing some general features to be expected for special cases of the parameters.

(i) The potential is uncoupled, that is

$$V(x, y) = V_x(x) + V_y(y), \tag{31}$$

whenever $\lambda a_{xy} = 0$. In this case, the Schrödinger equation is separable in Cartesian coordinates, and the wavefunctions and energies respectively are given by products and sums of their counterparts for one-dimensional anharmonic oscillators with potentials V_x and V_y.

(ii) The potential is symmetric, that is $V(x, y) = V(y, x)$, whenever $Z_x^2 = Z_y^2$ and $a_{xx} = a_{yy}$. In this case, the states $\phi_{j,k}$ and $\phi_{k,j}$ are degenerate. Moreover, parity can be used to classify the states; the parity of $\phi_{j,k}(x, y)$ is $(-1)^j$ for inversion with respect to x, and $(-1)^k$ for inversion in y.

(iii) The potential is radial, that is $V(x, y) = U(r)$ where $r^2 = x^2 + y^2$, whenever $Z_x^2 = Z_y^2 = Z^2$ and $a_{xx} = a_{yy} = a_{xy} = a$ because it can then be written as

$$V(x, y) = U(r) = -Z^2r^2 + \lambda ar^4/2. \tag{32}$$

In this case, the Schrödinger equation is separable in circular or polar coordinates, $\{r, \theta\}$, related to Cartesian coordinates by $x = r\cos\theta$ and $y = r\sin\theta$. Circular potentials are a subset of symmetric potentials, and hence display all the degeneracies associated with symmetric potentials. Further, the increased symmetry for radial potentials leads to additional degeneracies [3]. For example, the (1, 1), (2, 0) and (0, 2) states are degenerate.

Computations were made for 35 sets of parameters, and the (0, 0), (1, 0), (0, 1) and (1, 1) states were considered for all the sets. Since all potentials with $\lambda > 0$ are equivalent to potentials with $\lambda = 1$ and suitably scaled values of a_{xx}, a_{yy} and a_{xy}, we set $\lambda = 1$ hereafter. Test calculations led us to choose the dimensions of the spatial grid to be $N_x = N_y = 1951$, and the spatial step sizes to be $h_x = h_y = 0.005$. These choices give a spatial grid that works reasonably well for all the parameter sets; no attempt was made to optimize the spatial

Table 1. Parameters and energies of symmetric potentials with $\lambda = 1$.

No	$Z_x^2 = Z_y^2$	$a_{xx} = a_{yy}$	a_{xy}	E_{00}	$E_{10} = E_{01}$	E_{11}
1	5	5	5	0.898 434 452	2.783 664 73	5.209 161 76
2	5	25	25	2.844 666 80	6.890 458 75	11.711 978 0
3	5	50	50	3.864 219 91	9.155 707 77	15.392 046 1
4	5	100	100	5.084 631 31	11.904 199 8	19.889 208 3
5	20	5	5	−7.068 312 82	−6.709 656 05	−5.755 461 65
6	35	5	5	−26.556 349 5	−26.395 752 9	−25.917 846 8
10	20	1	1	−46.876 331 8	−46.823 759 0	−46.666 238 7
21	7/2	1	0	−1.089 914 92	−0.741 690 832	−0.393 466 740
22	10	1	0	−20.633 576 7	−20.633 561 8	−20.633 546 9
26	6	6/5	3/5	−2.823 368 92	−2.571 409 84	−2.198 792 65
27	10	3/2	3/4	−7.887 155 80	−7.810 351 99	−7.718 680 66
31	5	5/8	15/16	−3.069 865 89	−2.879 580 68	−1.986 011 29
32	8	5/8	15/16	−9.978 944 71	−9.947 40 478	−8.620 338 08

Table 2. Parameters and energies of asymmetric potentials with $\lambda = 1$.

No	Z_x^2	Z_y^2	a_{xx}	a_{xy}	a_{yy}	E_{00}	E_{10}	E_{01}	E_{11}
7	2	3	1/2	1/2	1/2	−0.786 751 007	0.027 616 271 9	−0.588 567 652	0.496 098 623
8	10	15	3/2	3/2	3/2	−14.975 793 4	−12.803 477 3	−14.975 787 6	−12.803 375 5
9	15	25	2	2	2	−34.009 151 9	−30.892 592 2	−34.009 151 9	−30.892 592 2
11	10	20	100	100	100	4.318 751 33	10.941 426 4	10.283 354 6	18.158 922 8
12	2	2	1/4	1/4	3/8	−0.938 852 500	−0.794 653 384	−0.415 569 926	−0.078 798 364 3
13	5	5	3/4	3/4	9/8	−2.403 033 75	−2.319 137 59	−1.644 430 57	−1.359 844 83
14	2	5	1/4	1/4	3/8	−6.215 377 46	−5.023 524 67	−6.215 305 04	−5.023 123 87
15	2	5	3/4	3/4	9/8	−0.890 373 704	0.240 646 297	−0.660 582 111	0.698 317 878
16	40	60	200	200	300	4.311 730 88	11.507 255 3	11.991 203 3	20.735 261 8
17	2	2	3/16	3/8	9/16	−1.091 197 60	−1.050 639 19	0.036 366 360 3	0.255 992 768
18	2	4	1/8	1/4	3/8	−3.637 223 50	−3.124 798 35	−3.626 942 37	−2.999 567 32
19	2	4	3/8	3/4	9/8	−0.532 779 073	0.000 229 393 878	0.041 418 254 5	0.972 395 418
20	15	25	50	100	150	3.803 941 99	8.671 973 79	10.686 033 9	16.960 176 1
23	3/2	2	1/2	0	1/2	−0.342 566 234	0.189 831 325	0.003 326 215 53	0.535 723 775
24	15	10	3	0	3	−8.935 664 37	−8.931 285 45	−8.791 028 37	−8.786 649 44
25	30	40	500	0	500	6.725 122 04	16.555 607 0	16.199 606 9	26.030 091 8
28	3	5	3/4	3/8	3/4	−2.427 111 83	−1.574 366 18	−2.388 089 83	−1.486 135 23
29	5	7	5/4	5/8	5/4	−3.057 356 20	−2.300 655 93	−2.997 528 73	−2.169 306 81
30	40	30	300	150	300	5.584 098 90	13.764 843 4	14.215 118 6	23.392 920 8
33	2	4	1/4	3/8	1/4	−5.664 392 66	−3.829 214 76	−5.664 358 72	−3.828 695 15
34	5	10	5/8	15/16	5/8	−16.259 155 8	−13.251 700 7	−16.259 155 8	−13.251 700 5
35	25	20	100	150	100	4.008 550 73	10.046 025 2	10.394 702 0	18.277 593 3

mesh for each parameter set. The time step varied from 0.0004 to 0.01 with smaller time steps generally needed for excited states. The convergence criterion for time propagation was $|E^{n+1} - E^n| < 10^{-12}$, and the number of time steps required to satisfy this criterion varied from a few hundred to a few thousand. Generally, using too large a time step leads to initially converging energies followed by divergence. Initial guesses were taken to be the simple, unnormalized forms

$$\psi_{0,0}^0 = \mathrm{e}^{-(x^2+y^2)}, \qquad \psi_{1,0}^0 = x\mathrm{e}^{-(x^2+y^2)} \qquad \psi_{0,1}^0 = y\mathrm{e}^{-(x^2+y^2)} \qquad \text{and} \qquad \psi_{1,1}^0 = xy\mathrm{e}^{-(x^2+y^2)}$$

The calculated energies are listed in tables 1 and 2 for symmetric and nonsymmetric potentials respectively. Energies previously published by Witwit and co-workers are available

Table 3. Expectation values and virial ratios R for selected potentials.

No	State	$\langle x^2\rangle$	$\langle y^2\rangle$	$\langle x^2y^2\rangle$	$\langle x^4\rangle$	$\langle y^4\rangle$	R
1	0, 0	0.259 6	0.259 6	0.058	0.175	0.175	0.999 99
1	1, 0	0.611 5	0.203 8	0.114	0.572	0.114	1.000 06
1	0, 1	0.203 8	0.611 5	0.114	0.114	0.572	0.999 99
1	1, 1	0.527 9	0.527 9	0.262	0.437	0.437	1.000 01
10	0, 0	4.919 3	4.918 5	12.5	37.5	37.5	0.999 80
10	1, 0	7.382 7	2.460 8	12.5	62.5	12.5	0.999 84
10	0, 1	2.460 9	7.382 6	12.5	12.5	62.5	0.999 88
10	1, 1	4.930 2	4.930 2	18.8	31.4	31.4	0.999 88
18	0, 0	0.867 9	4.332 2	2.98	2.40	22.6	1.000 02
18	1, 0	3.687 0	2.384 4	6.08	20.8	9.48	0.999 86
18	0, 1	0.766 2	4.439 6	2.92	1.76	23.4	1.000 00
18	1, 1	2.446 3	3.390 2	7.05	9.61	14.9	0.999 99
22	0, 0	4.764 8	4.764 8	22.7	24.9	24.9	0.999 83
22	1, 0	4.764 9	4.764 8	22.7	24.9	24.9	0.999 85
22	0, 1	4.764 8	4.764 9	22.7	24.9	24.9	0.999 89
22	1, 1	4.764 9	4.764 9	22.7	24.9	24.9	0.999 91
23	0, 0	0.871 7	1.207 1	1.05	1.69	2.82	0.999 96
23	1, 0	1.641 9	1.207 1	1.98	3.94	2.82	0.999 98
23	0, 1	0.871 7	1.912 8	1.67	1.69	5.16	0.999 98
23	1, 1	1.641 9	1.912 8	3.14	3.94	5.16	0.999 98
27	0, 0	1.977 2	1.977 2	3.47	5.30	5.30	0.999 79
27	1, 0	2.167 6	1.862 8	3.68	5.97	4.79	0.999 90
27	1, 1	2.068 0	2.068 0	3.99	5.48	5.48	0.999 91

for the parameter set 1 [7], the sets 13 and 26 [3], and the sets 10 and 22 [5]. Four of these five-parameter sets correspond to symmetric potentials, and there are a total of 16 unique energies to be compared. Their energies have to be divided by two to correspond to our values because their Hamiltonian is twice ours. For the parameter sets 1, 13 and 26 one has to recognize that their results are for potentials with $\lambda = 5, 3/2$ and $6/5$ with scaled values of the a_{ij} parameters. The mean unsigned error of our energies with respect to Witwit's values, which were computed with extended precision arithmetic, was 1.3×10^{-7}.

A check on the accuracy of our wavefunctions is provided by the virial theorem [23, 24] for bound stationary states,

$$\sum_i \langle q_i(\partial V/\partial q_i)\rangle = 2\langle T\rangle, \tag{33}$$

in which the q_i are Cartesian components of the position vectors and $\langle T\rangle$ is the expectation value of the kinetic energy. For the two-dimensional double-well problem under consideration, using equation (29), the virial theorem takes the form:

$$\langle\phi|x(D_xV)|\phi\rangle + \langle\phi|y(D_yV)|\phi\rangle = \langle D_x\phi|D_x\phi\rangle + \langle D_y\phi|D_y\phi\rangle. \tag{34}$$

A measure of the wavefunction error is therefore given by the deviation of the virial ratio

$$R = \frac{\langle\phi|x(D_xV)|\phi\rangle + \langle\phi|y(D_yV)|\phi\rangle}{\langle D_x\phi|D_x\phi\rangle + \langle D_y\phi|D_y\phi\rangle} \tag{35}$$

from its exact value of 1. Values of the virial ratio are listed in table 3 for a few selected parameter sets. For all the parameter sets and states considered, we found $0.999\,79 \leqslant R \leqslant 1.000\,06$ where the maximum deviation was for the ground state of potential 30.

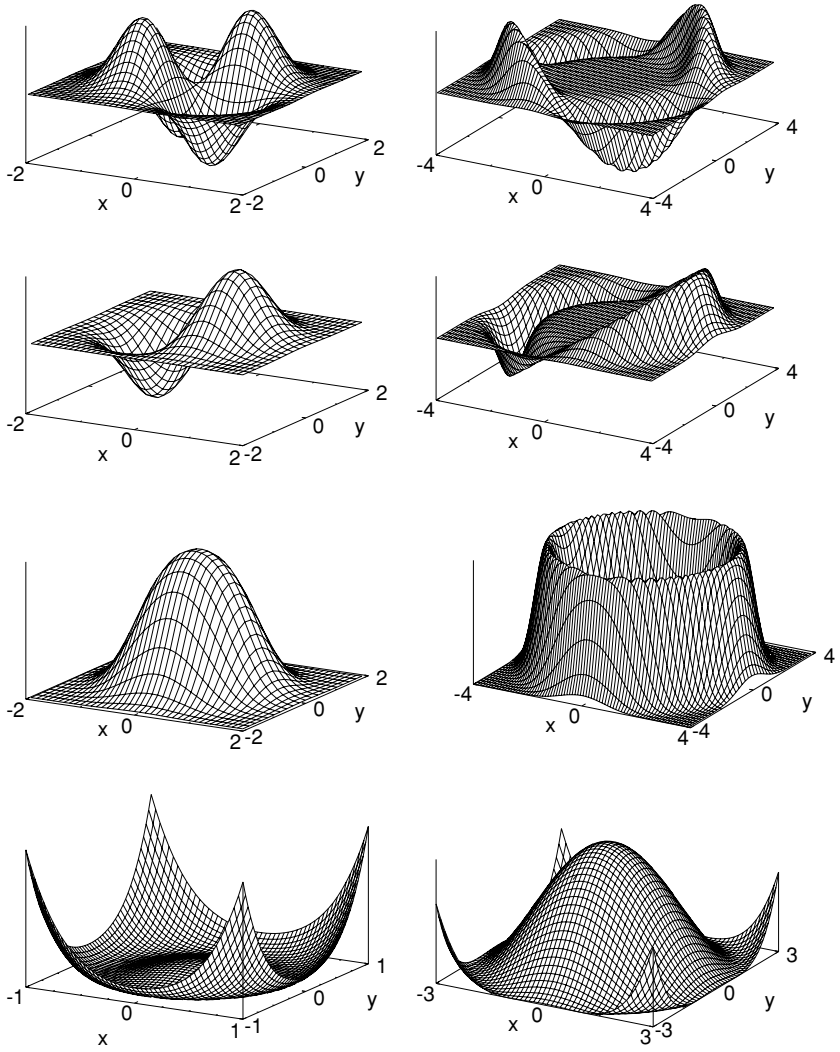

Figure 1. Potentials and wavefunctions for parameter sets 1 (left) and 10 (right). From bottom to top: V, ϕ_{00}, ϕ_{10} and ϕ_{11}.

For the symmetric potentials, we checked that the energies for the degenerate states (1, 0) and (0, 1) coincided to at least the number of significant figures shown in table 1. Several numerical checks can also be made using the expectation values listed in table 3. These checks are quite sensitive since the expectation values are likely to be significantly less accurate than the energies. For symmetric potentials, we should find $\langle x^k\rangle = \langle y^k\rangle$ for the (0, 0) and (1, 1) states, and $\langle x^k\rangle_{1,0} = \langle y^k\rangle_{0,1}$ and $\langle x^k\rangle_{0,1} = \langle y^k\rangle_{1,0}$ where the subscripts indicate the states. Table 3 shows that these checks hold up quite well with the largest deviation of 8×10^{-5} seen between $\langle x^2\rangle$ and $\langle y^2\rangle$ for the ground state of potential 10. For the uncoupled potentials, $\langle x^2y^2\rangle = \langle x^2\rangle\langle y^2\rangle$ as can be verified for potentials 22 and 23 in table 3.

As Z_x^2 and Z_y^2 increase, the potential wells become deeper, the barrier becomes more nearly impenetrable, the states get more localized in the wells and hence pseudo-degeneracies arise as observed previously [3, 5]. Pseudo-degeneracies in one-dimensional double wells are

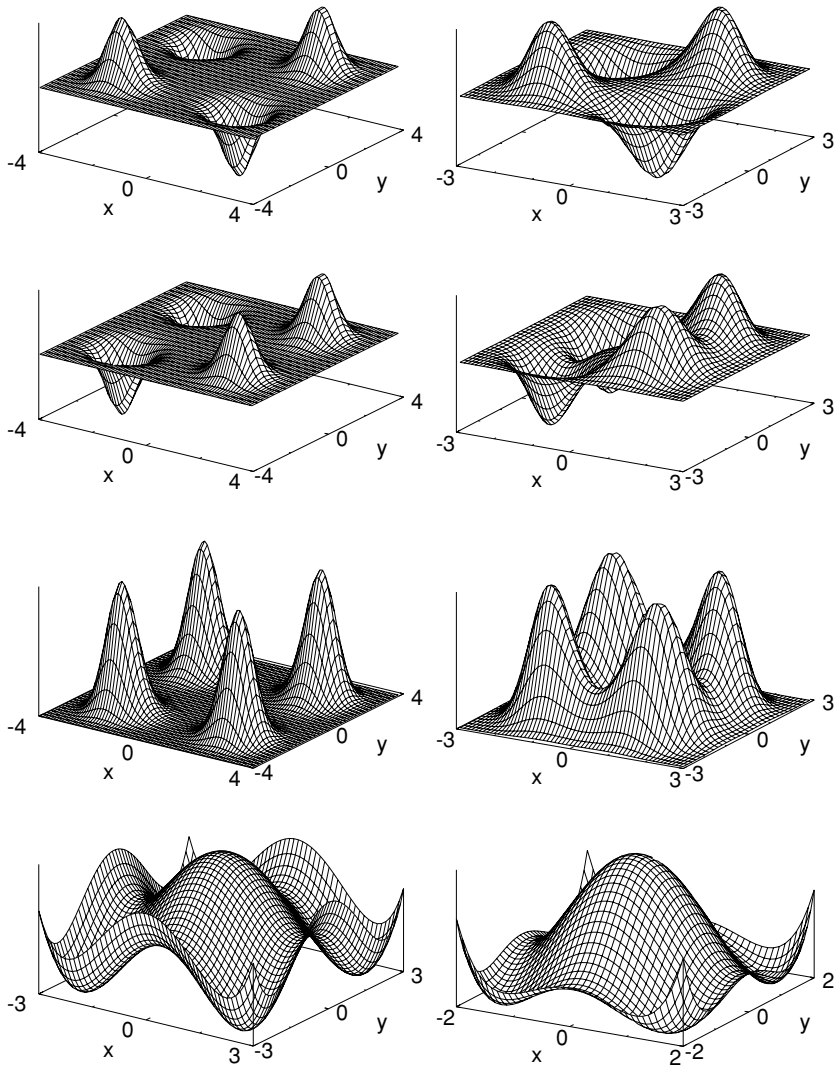

Figure 2. Potentials and wavefunctions for parameter sets 22 (left) and 27 (right). From bottom to top: V, ϕ_{00}, ϕ_{10} and ϕ_{11}.

well known [25, 13]. For symmetric potentials,

$$E_{00} \approx E_{10} = E_{01} \approx E_{11} \tag{36}$$

as seen for the potentials 10, 22 and 27 in table 1. For the nonsymmetric potentials, the energies split up into two near-degenerate pairs. One member of the pair (E_{10}, E_{01}) becomes nearly degenerate with E_{00} and the other with E_{11} as seen for parameter sets 8, 9, 14, 24, 33 and 34 in table 2. In fact, table 2 suggests that there are exact degeneracies for parameter sets 9 and 34. However, examining the energies to a greater number of significant figures reveals that $|E_{00} - E_{01}| \approx 7 \times 10^{-9}$ and $|E_{10} - E_{11}| \approx 3 \times 10^{-9}$ for potential 9, and $|E_{00} - E_{01}| \approx 1 \times 10^{-8}$ for potential 34.

The wavefunctions for parameter sets 1 and 10 are shown in figure 1. Both potentials are radial but potential 1 has a much smaller barrier height to well depth ratio than potential 10.

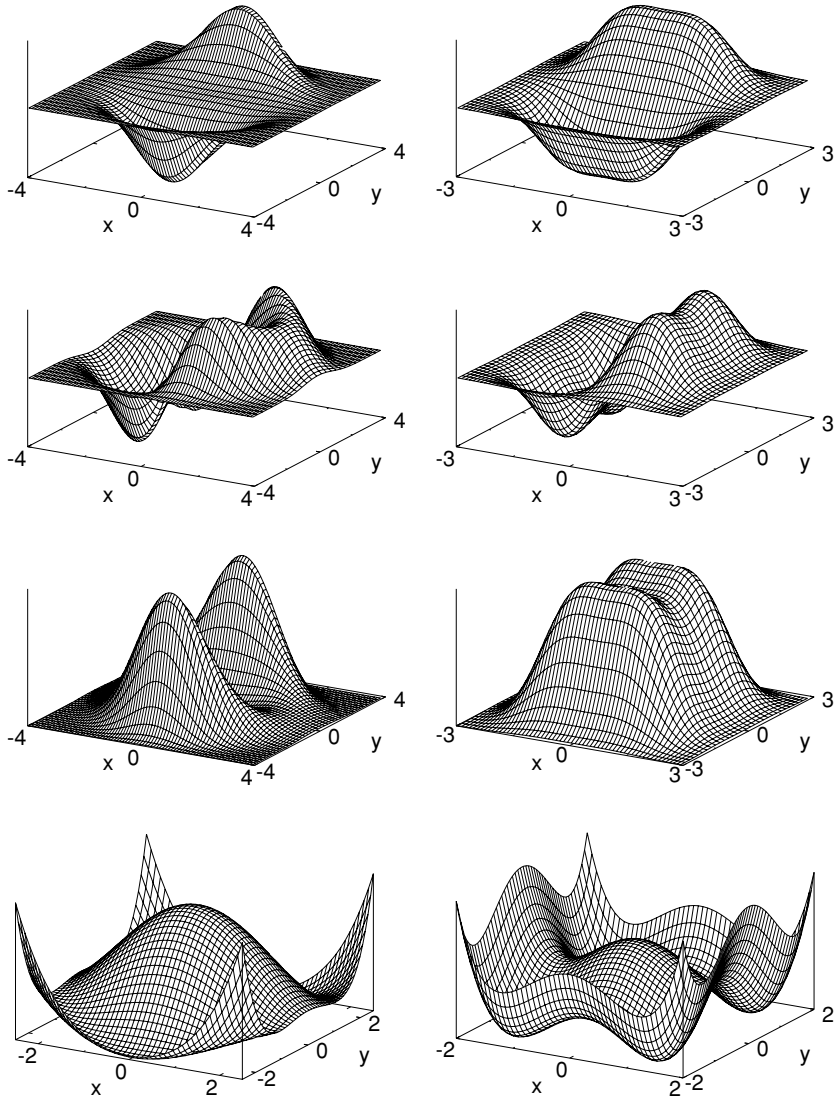

Figure 3. Potentials and wavefunctions for parameter sets 18 (left) and 23 (right). From bottom to top: V, ϕ_{00}, ϕ_{10} and ϕ_{01}.

Thus the wavefunctions show that probability density is scooped away from the central region for potential 10.

The wavefunctions for parameter sets 22 and 27 are shown in figure 2. Both potentials are symmetric, and potential 22 is uncoupled. In both cases, the wavefunctions show localization of the particle at points close to the locations of the four potential minima. However, the probability density in the regions between the wells is larger for potential 27 because it has a slightly smaller barrier height to well depth ratio.

Finally, consider the wavefunctions for parameter sets 18 and 23 shown in figure 3. Neither potential is symmetric, and potential 23 is uncoupled. Potential 18 has two wells at $x = 0$, $y = \pm 2.3$, whereas potential 23 has four wells at $x = \pm 1.22$, $y = \pm 0.71$. In both cases,

the ground-state wavefunction shows localization of the particle close to the locations of the potential minima. However, the probability density in the regions between the wells is larger for potential 23 because it has a smaller barrier height to well depth ratio than potential 18.

5. Concluding remarks

The finite-difference method described provides another route to the bound state energies and wavefunctions of two-dimensional double wells. The wavefunction plots have led to greater appreciation of localization and delocalization in these systems.

Improved accuracy can be obtained by the use of higher precision arithmetic, spatial grids optimized for each potential, better initial wavefunctions and higher-order finite-difference methods. Such improvements and applications to different potential functions would be interesting.

Acknowledgment

The Natural Sciences and Engineering Research Council of Canada supported this work.

References

[1] Hund F 1927 *Z. Phys.* **43** 805–26
[2] Witwit M R M 1993 *J. Math. Phys.* **34** 5050–61
[3] Witwit M R M and Killingbeck J P 1995 *Can. J. Phys.* **73** 632–7
[4] Witwit M R M 1996 *J. Math. Chem.* **20** 273–83
[5] Witwit M R M 1996 *J. Comput. Phys.* **123** 369–78
[6] Witwit M R M and Gordon N A 1997 *Can. J. Phys.* **75** 705–14
[7] Witwit M R M 1997 *J. Math. Chem.* **22** 11–23
[8] Witwit M R M 1998 *J. Math. Chem.* **24** 249–59
[9] Witwit M R M and Gordon N A 1998 *Can. J. Phys.* **76** 609–20
[10] Metropolis N and Ulam S 1949 *J. Am. Stat. Assoc.* **44** 335–41
[11] Anderson J B 1975 *J. Chem. Phys.* **63** 1499–503
[12] Hammond B L, Lester W A Jr and Reynolds P J 1994 *Monte Carlo Methods in Ab Initio Quantum Chemistry* (Singapore: World Scientific)
[13] Roy A K, Gupta N and Deb B M 2001 *Phys. Rev.* A **65** 012109
[14] Gupta N, Roy A K and Deb B M 2002 *Pramana* **59** 575–83
[15] Wadhera A, Roy A K and Deb B M 2003 *Int. J. Quantum Chem.* **91** 597–606
[16] Killingbeck J 1985 *J. Phys. A: Math. Gen.* **18** 245–52
[17] Neuhauser D 1990 *J. Chem. Phys.* **93** 2611–6
[18] Peaceman D W and Rachford H H 1955 *J. Soc. Ind. Appl. Math.* **3** 28–41
[19] Thomas J W 1995 *Numerical Partial Differential Equations: Finite Difference Methods* (New York: Springer)
[20] Deb B M and Chattaraj P K 1989 *Phys. Rev.* A **39** 1696–713
[21] Abramowitz M and Stegun I (ed) 1968 *Handbook of Mathematical Functions* (New York: Dover)
[22] Dahlquist G and Björck Å 1974 *Numerical Methods* (London: Prentice-Hall)
[23] Fock V A 1930 *Z. Phys.* **63** 855–8
[24] Levine I N 2000 *Quantum Chemistry* 5th edn (Englewood Cliffs, NJ: Prentice-Hall)
[25] Banerjee K and Bhatnagar S P 1978 *Phys. Rev.* D **18** 4767–9